

Adaptive Adversarial Attack on Scene Text Recognition

Xiaoyong Yuan^{1,3}, Pan He¹, and Xiaolin Andy Li^{2,3}

¹ Dept. of CISE, University of Florida

² Dept. of ECE, University of Florida

³ Large-scale Intelligent Systems Laboratory, University of Florida

Abstract. Recent studies have shown that state-of-the-art deep learning models are vulnerable to the inputs with small perturbations (adversarial examples). We observe two critical obstacles in adversarial examples: (i) Strong adversarial attacks require manually tuning hyper-parameters, which take longer time to construct a single adversarial example, making it impractical to attack real-time systems; (ii) Most of the studies focus on non-sequential tasks, such as image classification and object detection. Only a few consider sequential tasks. Despite extensive research studies, the cause of adversarial examples remains an open problem, especially on sequential tasks. We propose an adaptive adversarial attack, called AdaptiveAttack, to speed up the process of generating adversarial examples. To validate its effectiveness, we leverage the scene text detection task as a case study of sequential adversarial examples. We further visualize the generated adversarial examples to analyze the cause of sequential adversarial examples. AdaptiveAttack achieved over 99.9% success rate with 3 ~ 6× speedup compared to state-of-the-art adversarial attacks.

Keywords: adversarial examples, multi-task learning, scene text recognition, deep learning

1 Introduction

Deep learning has drawn increasing attention on various tasks such as image recognition [1,2], object detection [3,4,5,6], speech recognition [7] and achieved state-of-the-art performance. However, prior studies [8,9,10,11] have shown that deep neural networks are vulnerable to *adversarial examples*, by adding imperceptible perturbations on original images to fool a deep learning model. Although there have been considerable studies and substantial interests in the phenomenon of adversarial examples, the optimization of generating adversarial examples and the sequential adversarial examples remain critical open problems in the community.

Many strong iterative optimization-based attacks [12,11,13] have been proposed to generate adversarial examples of high-quality. They are hard to defend by most defensive mechanisms [14,13]. However, these iterative methods usually

require longer time/more iterations to find proper weights, which becomes an obstacle to applying adversarial attacks to real-time systems. For example, it takes about one hour to generate single adversarial audio with a few seconds [15].

Multi-task optimization: Generating adversarial examples is inherently a multi-task optimization problem, where we try to minimize distances between original examples and adversarial examples while minimizing the classification loss (e.g., cross-entropy loss, CTC loss [16]) of adversarial examples on targeted labels. Previous works simultaneously optimize both of the two objectives, by using a naïve weighted sum of multi-task losses. The weights of losses are uniformly set [12] or manually tuned [11]. For example, Carlini and Wagner [11] used a modified binary search to find a proper weight to generate adversarial examples.

However, the optimal weights between two tasks are strongly dependent on tasks (e.g., image distance vs. audio distance, cross-entropy loss vs. CTC loss). Researchers and practitioners have to carefully choose appropriate weights between task losses to achieve a good performance. Therefore, *it is desirable to find a better approach to learn the optimal weights automatically.*

Multi-task learning is widely studied in many machine learning tasks. Recently, Kendall et al. [17,18] learned multi-task weightings by combining observation (*aleatoric*) uncertainty and model (*epistemic*) uncertainty and modeled each task in a unified Bayesian deep learning framework. This approach outperformed the equivalent separately trained models. We assume that the two tasks in adversarial attacks (minimizing the classification loss and adversarial perturbations) follow probabilistic models. Inspired by [17], we firstly focus on attacking general (non-sequential) classification problem by adaptively balancing tasks and tuning the weights. We refer to this method as *AdaptiveAttack*. However, applying the idea to sequential classification tasks is non-trivial, due to the specific objective function for sequential learning. Sequential learning involves automatic segmentation of the sequence (decoding), which transforms the network outputs into a conditional probability distribution over label sequences. In addition to non-sequential problem, we need to tackle the numerous decoding paths before applying *AdaptiveAttack* to sequential learning problems.

Adversarial attack on sequential learning: Current studies on adversarial examples mainly focus on non-sequential adversarial classification problems, including tasks such as image classification [8,9,10], face recognition [19], reinforcement learning on image inputs [20,21], object detection [22], and semantic segmentation [23,24]. Only very few targets at sequential labeling tasks, such as speech-to-text [25,15] and reading comprehension [26,27], not to mention the cause of sequential adversarial examples. Even for non-sequential classification tasks, the cause of adversarial examples has not been well explained and visualized, although there have been several promising hypotheses [9,28,29,30,31].

The differences between non-sequential and sequential adversarial examples involve the following aspects: (i) The output of a sequential model is usually a varied-length label, instead of a single label. When generating adversarial examples, the non-sequential model (such as object classification model) only involves

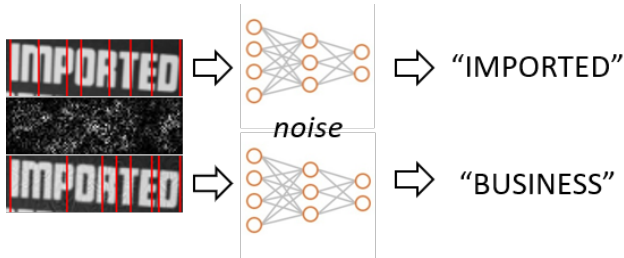


Fig. 1: An adversarial example of the scene text recognition system. First row: an original image from the *ICDAR* dataset, predicted as ‘IMPORTED’. Second row: adversarial perturbations added on the original image. Third row: the adversarial image, which is incorrectly predicted as ‘BUSINESS’. Humans can barely recognize the difference between these two images. Red lines denote the CTC alignment outputs of the image.

the *substitution* operation (e.g. modify the original class label), while the sequential model (such as speech-to-text model) considers three operations: *insertion*, *substitution*, and *deletion* (e.g. insertion: coat \rightarrow coats, substitution: coat \rightarrow cost, deletion: coat \rightarrow cot). (ii) Each character in target labels needs to be well-aligned. In the sequential model, the requirement of the alignment between input and output poses a challenge on generating adversarial examples. (iii) Different from non-sequential models, sequential models usually leverage recurrent neural networks, where the internal feature representation involves more sequential context than those in convolutional neural networks.

Inspired by these observations, in this paper, we select scene text recognition as a case study to investigate the cause of sequential adversarial examples. The scene text recognition task is naturally a sequential learning problem, which is closely related to standard classification problems in computer vision tasks. Measuring hidden features in the object classification task or speech recognition task is difficult, with more uncertainty on model interpretability. We instead choose to attack a scene text recognition model by modifying each character in the text image, due to more intuitive explanations on how the perturbations affect the final output. Figure 1 illustrates an adversarial example of a scene text recognition system.

1.1 Contributions

- We propose a novel *AdaptiveAttack* that directly learns multi-task weightings without manually searching hyper-parameters compared with the previous adversarial attacks. *AdaptiveAttack* is a general method, which can be applied to the existing iterative optimization-based attacks for both non-sequential and sequential tasks. In our experiments, *AdaptiveAttack* accelerates the whole process of generating adversarial examples by three to six times.
- We successfully attack a scene text recognition system with over 99.9% success rate on several benchmark datasets. To the best of our knowledge, it is

the first work to generate adversarial examples on a scene text recognition system.

- We visualize the generated adversarial examples on the sequential learning with CTC alignments and investigate the cause of the sequential adversarial phenomenon.

2 Background

2.1 Connectionist Temporal Classification

Connectionist Temporal Classification (CTC) [16] is specifically designed for training sequence-to-sequence neural network on sequential classification tasks, where the alignment between the inputs and the target labels is unknown. CTC aims at transforming the network outputs into a conditional probability distribution over label sequences and selects the most probable labeling for a given input sequence. We briefly introduce CTC in this section. We will later generate adversarial examples based on CTC algorithm.

Let \mathcal{X} be the input domain - a single frame of input - and \mathcal{Y} be the range - the (finite) alphabet \mathcal{S} of labels plus a blank label. For an input sequence of T frames $x_t \in \mathcal{X}$, the network will output a probability distribution over the output domain for each frame, where we denote the mapping function as \mathcal{F} . Denote by y_k^t the activation of output unit $k \in \mathcal{Y}$ at frame t and y_k^t is then interpreted as the probability of observing label k at frame t . We use π to denote one path: a sequence of characters $y_{\pi_t}^t, \pi_t \in \mathcal{Y}$.

While \mathcal{F} maps every frame to a probability distribution over the characters, this does not directly give us a probability distribution over all paths. To achieve this, we define a label l , which can be obtained by removing all blanks and repeated labels from the path π (e.g., $\mathcal{B}(a-ab) = \mathcal{B}(-aa-abb) = aab$). Given an input sequence X , the probability of a given path π can be written as:

$$\Pr(\pi|x) = \prod_{t=1}^T y_{\pi_t}^t \quad (1)$$

We use \mathcal{B} to define the conditional probability of a given labeling l . We then sum up the probabilities of all the paths:

$$\Pr(l|x) = \sum_{\pi \in \mathcal{B}^{-1}(l)} \Pr(\pi|x) \quad (2)$$

It is numerically stable to calculate the probability by negative log likelihood: $CTC_{Loss}(x, l) = -\log \Pr(l|x)$. Given the above formulation, the output of the classifier should be the most probable labeling for the input sequence:

$$h(X) = \arg \max_{l \in \mathcal{S}^T} \Pr(l|x). \quad (3)$$

Because computing $h(x)$ requires searching an exponential space, we typically approximated the $h(x)$ in one of two ways. The first method (Greedy Path Decoding) is based on the assumption that the most probable path will correspond to the most probable labeling:

$$h(x) \approx \mathcal{B}(\pi^*)$$

$$\text{where } \pi^* = \arg \max_{\pi \in \mathcal{Y}^T} P(\pi|x) \quad (4)$$

The other method (Beam Search Decoding) simultaneously evaluates the likelihood of multiple alignments π and then chooses the most likely path ρ under these alignments. In our experiment, we use Greedy Path Decoding for simplicity.

2.2 Scene Text Recognition

Scene text recognition tasks aim at decoding a sequence of text characters from a cropped but variable-length word image. Prior to the use of neural networks, previous studies focus on developing individual character classifiers, following the pipeline of conventional OCR techniques: a character-level segmentation, then an isolated character classifier and post-processing for final recognition. However, their performance was severely limited by the character segmentation. More importantly, recognizing individual character with finite-length context sliding windows discards meaningful context information between characters, reducing the model’s reliability and robustness.

Apart from character-level approaches, most recent text recognition approaches focus on mapping the entire image to a word string directly, either with hand-crafted features or deep learning features. Almazán [32] proposed a subspace regression method to jointly embed both word images and their text strings into a common subspace, resulting in solving a nearest neighbor problem. Jaderberg, et al. [33] developed a CNN model to cast the word recognition into a multi-class classification problem. They further proposed a CNN based architecture, incorporating a Conditional Random Field (CRF) graphical model for unconstrained text recognition [34]. Su, et al. [35] built a RNN with HOG features and casted text recognition as a sequence labeling problem. He, et al. [36] and Shi, et al. [37] extracted rich visual features from a CNN, then a sequence labeling is carried out with LSTM [38] and CTC [16]. Lee [39] incorporated attention modeling into recursive recurrent neural networks for lexicon-free optical character recognition in natural scene images. Shi, et al. [40] and Liu, et al. [41] extend the work of [42] to transform a distorted text region into a canonical pose suitable for recognition. In our experiment, we train a similar recognition model, based on the state-of-the-art approach, Convolutional Recurrent Neural Network (CRNN) [37].

2.3 Adversarial Examples

Adversarial examples are imperceptible to human but can easily fool deep neural networks in the testing/deploying stage. People have studied adversarial ex-

amples on machine learning models (machine learning evasion attacks) since 2012 [43]. Adversarial examples at the training stage (data poisoning) is another interesting topic, but we will not discuss it in the paper.

With rapid progress and great success in a wide spectrum of applications, deep learning is being applied in many safety-critical environments. The vulnerability to adversarial examples becomes one of the major obstacles for applying deep neural networks in safety-critical scenarios. Most existing studies on adversarial examples focus on computer vision related tasks: image classification [8,9,10], face recognition [19], reinforcement learning [20,21], object detection [22], and semantic segmentation [23,24]. Only a few studies have been devoted to sequential domains, such as speech recognition [25,15] and reading comprehension [26,27].

Iterative attacks have been prevalent in generating adversarial examples due to their high success rate and small perturbations: iteratively searching and updating the perturbations based on the gradient of the output of the victim model. In contrast, one-time attacks only update the adversarial perturbations once, so that performance of one-time attacks is worse than iterative ones. Researchers currently apply one-time attacks on real-time systems. For example, [20,21] leveraged a one-time attack, Fast Gradient Sign Method (FGSM) [9], to attack reinforcement learning systems due to the requirement of quick response to the real-time input. However, it is easy to detect/defend one-time attacks.

The magnitude of perturbations is usually measured by ℓ_p norm ($p = 0, 1, \infty$). A few studies use other measurements (e.g., SSIM [44], spatial transformation [45]) [46] analyzed the suitability of these measurements. In this paper, we only consider ℓ_2 norm, which can be comparable to most of the existing work. For further details on adversarial attacks, we refer to [47]. To our best knowledge, we are the first group to successfully generate sequential adversarial examples on a scene text recognition system.

3 Proposed Sequential Adversarial Attack (AdaptiveAttack)

In this section, we first introduce our sequential attack on a scene text recognition system. To avoid manually tuning task weights in the sequential attack, we then propose an adaptive method, *AdaptiveAttack* to generate adversarial examples on both non-sequential and sequential classification problems.

3.1 Threat Model

We assume that the adversary has access to the scene text recognition system, including the architecture and parameters of the recognition model. This type of attack is referred to “White-Box Attack”. We do not consider the “Black-Box Attack” in this paper, which assumes the adversary has no access to the trained neural network model. Prior work has shown that adversarial examples generated by “White-Box Attack” can be transferred to attack black-box services due to

the transferability of adversarial examples [48]. Approximating the gradients [49] is another option to make a “Black-Box Attack”.

Our attack fools the scene text recognition system by predicting a specific (targeted) sequence of text instead of an arbitrary (non-targeted) one. These two types of attacks are usually called *targeted attack* and *non-targeted attack*. Non-targeted attacks are much easier to be conducted than targeted attacks [47].

3.2 Basic Attack

Give an input image x , the ground-truth sequential label $l = \{l_0, l_1, \dots, l_T\}$, a targeted sequential label $l' = \{l'_0, l'_1, \dots, l'_{T'}\}$ ($l \neq l'$), and a well-trained scene text recognition model \mathcal{F} , we formulate the problem of generating adversarial examples as the following optimization problem:

$$\begin{aligned}
 & \underset{x'}{\text{minimize}} && \mathcal{D}(x, x') \\
 & \text{s.t.} && \mathcal{F}(x') = l', \\
 & && \mathcal{F}(x) = l, \\
 & && x' \in [-1, 1]^n,
 \end{aligned} \tag{5}$$

where x' is the modified adversarial image. $x' \in [-1, 1]^n$ ensures the adversarial image is a valid input. $\mathcal{D}(\cdot)$ denotes the distance between the original image and the adversarial image.

Following C&W Attack [11], we transform the function \mathcal{F} to a differentiable function, CTC_{Loss} . To remove the constraint of validation on new input x' , we introduce a new variable w to replace x' , where $x' = \tanh(w)$. The new optimization problem can be written as:

$$\underset{x'}{\text{minimize}} \quad CTC_{Loss}(\tanh(w), l') + \lambda \mathcal{D}(x, \tanh(w)), \tag{6}$$

where $CTC_{Loss}(\cdot, \cdot)$ denotes the CTC loss of the classifier \mathcal{F} . λ is a hyperparameter to balance the importance of being adversarial and close to the original image. λ is a task and data dependent parameter. People usually search for a proper λ uniformly (log scale). In the experiment, we follow a modified binary search between $\lambda = 0.01$ and $\lambda = 1000$, starting from $\lambda = 0.1$. For each λ , we run 2,000 iterations of gradient descent searching using Adam [50], a stochastic optimizer. We adopt an early stop mechanism to avoid unnecessary computation.

3.3 AdaptiveAttack

It is time-consuming to search for λ manually and find an optimal parameter λ , since λ largely depends on individual tasks. In our experiment (Section 4.2), we compare the performance of Basic Attack with fixed λ values, regarding the success rate of attacks, the iterations of gradient search, and the magnitude of perturbations (Figure 2). We cannot find a proper value of fixed λ that achieves a high success rate, small iterations, and small perturbations simultaneously. For

modified binary searching of λ , as long as we conduct enough searching steps, it can always find a proper λ to achieve high success rate and small perturbations. However, it takes much longer time, which makes adversarial examples hardly applicable to real-time systems.

Inspired by [17], we propose an adaptive search method. *AdaptiveAttack*, to generate adversarial examples. From Equation 6, CTC loss $CTC_{Loss}(\cdot, \cdot)$ and Euclidean loss $\mathcal{D}(\cdot, \cdot)$ are viewed as a classification task and a regression task respectively. Thus generating adversarial examples (Equation 6) becomes solving a multi-task problem with two objectives.

First, we consider non-sequential classification tasks. We optimize the adversarial images based on maximizing the Gaussian likelihood with uncertainty:

$$\text{maximize } \Pr(x'|x, l') \quad (7)$$

We assume that $\Pr(x')$ and $\Pr(x, l')$ are constant values, and x and l' are independent variables, then

$$\begin{aligned} \Pr(x'|x, l') &= \frac{\Pr(x, l'|x') \cdot \Pr(x')}{p(x, l')} \\ &\propto \Pr(x, l'|x') \\ &= \Pr(x|x') \Pr(l'|x') \end{aligned} \quad (8)$$

We define original input x as a Gaussian distribution with mean given by x' and a noise scale λ_1 :

$$\Pr(x|x') = \mathcal{N}(x', \lambda_1^2). \quad (9)$$

The log likelihood function can be written as:

$$\log \Pr(x|x') \propto -\frac{\|x - x'\|_2^2}{2\lambda_1^2} - \log \lambda_1^2. \quad (10)$$

For a classification problem, we apply a classification likelihood to the output:

$$\Pr(l'|x') = \text{Softmax}(f(x')), \quad (11)$$

where $f(\cdot)$ denotes the output of neural network before softmax layer. We adapt a squashed version of model output with a positive scalar λ_2 :

$$\begin{aligned} \Pr(l'|x', \lambda_2) &= \text{Softmax}\left(\frac{f(x')}{\lambda_2}\right), \\ \log \Pr(l' = c|x', \lambda_2) &= \frac{f_c(x')}{\lambda_2} - \log \sum_{c'} \exp \frac{f_{c'}(x')}{\lambda_2} \end{aligned} \quad (12)$$

Then we define the joint loss (optimized objective) as follows:

$$\begin{aligned} \mathcal{L} &= -\log \Pr(x, l'|x') \\ &= -\log \Pr(x|x') - \log \Pr(l'|x') \end{aligned} \quad (13)$$

According to [17], we can derive the optimization problem (Equation 7,8) by minimizing:

$$\mathcal{L} \propto \frac{\mathcal{L}_1(x, x')}{2\lambda_1^2} + \frac{\mathcal{L}_2(x', l')}{\lambda_2^2} + \log \lambda_1^2 + \log \lambda_2^2, \quad (14)$$

where $\mathcal{L}_1(x, x') = \|x - x'\|_2^2$ denotes the squared Euclidean loss and $\mathcal{L}_2(x, l')$ denotes the cross-entropy loss. Thus, we can adaptively generate adversarial examples for general (non-sequential) classification tasks without tuning parameter λ by hand.

Second, we consider sequential classification tasks. We propose a new method to solve sequential adversarial tasks adaptively. We define the likelihood of a sequential classification task following a Gaussian distribution, which sums up the probability of all possible valid paths based on targeted sequential output: According to Equation 2, the log likelihood function can be written as:

$$\log \Pr(l'|x') = \log \sum_{\pi \in \mathcal{B}^{-1}(l')} \Pr(\pi|x') \quad (15)$$

Here, we only consider paths with probability greater than or equal to a small constant c : $\Pr(\pi|x') = \prod_{t=1}^T y_{\pi_t}^t \geq c$. Suppose only two valid paths satisfy this constraint: π_1, π_2 .

$$\begin{aligned} -\log \Pr(l'|x') &\approx -\log (\Pr(\pi_1|x') + \Pr(\pi_2|x')) \\ &\leq -\frac{\log \Pr(\pi_1|x') + \log \Pr(\pi_2|x')}{2} - \log 2 \quad (\text{Jensen's Inequality}) \\ &= -\frac{1}{2} \log \prod_{t=1}^T \Pr(y_{\pi_{1t}}^t) - \frac{1}{2} \log \prod_{t=1}^T \Pr(y_{\pi_{2t}}^t) - \log 2 \\ &= -\frac{1}{2} \sum_{t=1}^T (\log \Pr(y_{\pi_{1t}}^t) + \log \Pr(y_{\pi_{2t}}^t)) - \log 2 \\ &\approx \frac{1}{2} \sum_{t=1}^T \left(-\frac{A_{1,t}}{\lambda_2^2} + \log \lambda_2^2 - \frac{A_{2,t}}{\lambda_2^2} + \log \lambda_2^2 \right) - \log 2 \\ &(\text{Similar to Equation 12}) \\ &= -\frac{\sum_{t=1}^T A_{1,t} + A_{2,t}}{2\lambda_2^2} + T \log \lambda_2^2 - \log 2, \end{aligned} \quad (16)$$

where $A_{i,t} = \log \text{Softmax}(y_{\pi_{it}}^t, f(x'))$, $i = 1, 2$.

The negative log likelihood of CTC Loss approximately equals to:

$$\begin{aligned} CTC_{Loss} &\approx -\log (\Pr(\pi_1|x') + \Pr(\pi_2|x')) \\ &= -\log \Pr(\pi_1|x') - \log \Pr(\pi_2|x') - \log \frac{\Pr(\pi_1|x') + \Pr(\pi_2|x')}{\Pr(\pi_1|x') \Pr(\pi_2|x')} \\ &\geq -\log \Pr(\pi_1|x') - \log \Pr(\pi_2|x') - \log \frac{2}{c}. \end{aligned} \quad (17)$$

Combining Equation 16 and 17, we have an upper bound of $-\log \Pr(l'|x')$ and the joint loss \mathcal{L} :

$$\begin{aligned}
 -\log \Pr(l'|x') &\leq \frac{CTC_{Loss} + \log \frac{2}{c}}{2\lambda_2^2} + T \log \lambda_2^2 - \log 2, \\
 \mathcal{L} &\leq \frac{\mathcal{L}_1(x, x')}{2\lambda_1^2} + \frac{CTC_{Loss}(x', l')}{2\lambda_2^2} + \log \lambda_1^2 + T \log \lambda_2^2 + \frac{1}{\lambda_2^2} - \log 2.
 \end{aligned} \tag{18}$$

To extend the number of valid paths from 2 to an arbitrary number n , the joint loss \mathcal{L} satisfies:

$$\mathcal{L} \leq \frac{\mathcal{L}_1(x, x')}{2\lambda_1^2} + \frac{CTC_{Loss}(x', l')}{n\lambda_2^2} + \log \lambda_1^2 + T \log \lambda_2^2 + \frac{\log n - (n-1) \log c}{n\lambda_2^2}. \tag{19}$$

From our observation, CTC loss always reduces very fast (Figure 4). Thus we can use a small number of valid paths to generate adversarial examples. From our experiments, it works well when $n < 50$. In this paper, we use $n = 2$ to report our results. Thus we can generate sequential adversarial examples by minimizing the upper bound of \mathcal{L} :

$$\text{minimize } \frac{\mathcal{L}_1(x, x')}{\lambda_1^2} + \frac{CTC_{Loss}(x', l')}{\lambda_2^2} + \log \lambda_1^2 + T \log \lambda_2^2 + \frac{1}{\lambda_2^2}. \tag{20}$$

4 Experiment and Analysis of Sequential Adversarial Examples

In this section, we generate adversarial examples on a scene text recognition model. We compare the performance of Basic Attack and propose AdaptiveAttack on three standard benchmarks. We then conduct experiments on a simulated sequential MNIST dataset and visualize the attack patterns on the generated adversarial examples.

4.1 Experiment Setup

We conducted experiments on three standard benchmarks for cropped word image recognition, namely the Street View Text dataset (SVT) [51], the ICDAR 2013 dataset (IC13) [52] and the IIIT 5K-word dataset (IIIT5K) [53]. The SVT dataset has 647 test word images collected from Google Street View of road-side scenes. The IC13 dataset contains 1015 test word images. The IIIT5K dataset is comprised of 5,000 cropped word images from both scene and born-digital images, with subsets of 2,000 and 3,000 images for training and test respectively. We train an end-to-end deep learning model using Pytorch, based on the state-of-the-art scene text recognition approach, Convolutional Recurrent Neural Network (CRNN) [37]⁴. We get the similar performance on the three benchmark datasets.

⁴ we refer to the implementation on <https://github.com/bgshih/crnn>, but modify the kernel size in the pooling layers to a get better alignment of output.

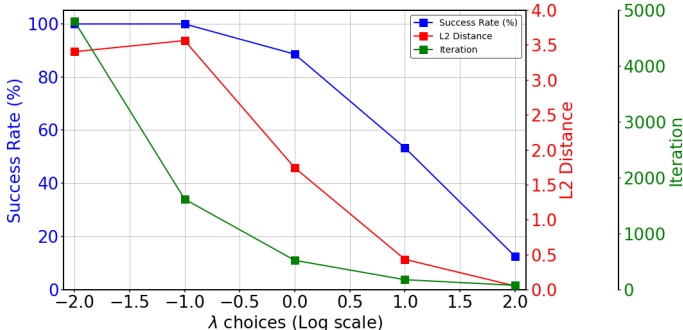


Fig. 2: **Performance of Basic Attack with fixed λ values.** We generate adversarial examples on the *ICDAR* dataset using Basic Attack. We run gradient descent searches for 10,000 iterations with fixed λ values (e.g., 0.01, 0.1, 1, 10, 100). Early stopping is adopted with 10-iteration tolerance to avoid unnecessary computation. None of the attacks with fixed λ values can well balance CTC loss (success rate curve in blue) and distance (L2 distance curve in red). It will take much larger iterations (iteration curve in green) to optimize the joint loss when we use a small λ . (We only calculate the successful adversarial examples for L2 distances and iterations to avoid the extremely large values when the attack fails.)

4.2 Basic Attack vs. AdaptiveAttack

We generate adversarial examples on the SVT, ICDAR, and IIIT5K dataset using Basic Attack and AdaptiveAttack. We set the targeted sequential label as the common word with the same length as the original one. For example, we replace the original label “this” with a targeted one “that”. The words used in the experiments are listed as follows: ‘a’, ‘of’, ‘the’, ‘that’, ‘about’, ‘search’, ‘contact’, ‘business’, ‘available’, ‘university’, ‘information’, ‘professional’, ‘international’, ‘administration’, ‘recommendations’, ‘responsibilities’, ‘interdisciplinary’, ‘telecommunications’.

Figure 2 shows the performance of Basic Attack with fixed λ values. When we use large values of λ (1, 10, 100), it fails to generate adversarial examples in most cases. For small values of λ (0.1, 0.01), although Basic Attack can successfully generate adversarial images, it spends much longer time and the magnitude of perturbations is much larger.

We then compare the performance of Adaptive Attack and Basic Attack using a fixed λ or a modified binary search. Table 1 lists our results. *Basic0.1*, *Basic1*, and *Basic10* denote Basic Attack with fixed λ values: 0.1, 1, and 10 respectively. *BasicBinary3*, *BasicBinary5*, *BasicBinary10* denote Basic Attack with 3, 5, and 10 steps of binary searching. We set the initial λ as 0.1, which is the best λ according to the results of fixed λ values (Figure 2). *Adaptive* denotes AdaptiveAttack.

Table 1: Performance Comparison between Basic Attack and AdaptiveAttack

Methods	ICDAR			SVT			IIIT5K		
	Success Rate	Distance	Iteration	Success Rate	Distance	Iteration	Success Rate	Distance	Iteration
Basic0.1	99.90%	3.57	1621.88	99.69%	3.59	1470.29	99%	2.90	7127.92
Basic1	88.55%	1.75	526.92	91.55%	1.67	518.99	95.39%	1.77	3606.26
Basic10	53.38%	0.44	179.75	68.23%	0.47	172.82	39.12%	0.39	1395.99
BasicBinary3	100.00%	1.64	1531.84	100.00%	1.17	1442.86	100.00%	2.01	4097.52
BasicBinary5	100.00%	1.64	1706.18	100.00%	1.15	1616.35	100.00%	1.96	5055.21
BasicBinary10	100.00%	1.58	2138.86	100.00%	1.11	1993.47	100.00%	1.94	6811.86
Adaptive	100.00%	2.15	480.28	100.00%	1.26	529.90	99.96%	2.68	682.48

From Table 1, we observe that both AdaptiveAttack and Basic Attack with a modified binary search can successfully generate adversarial examples on the scene text recognition model. Basic Attack with fixed λ values cannot achieve either high success rate or low distance of perturbations. AdaptiveAttack conducts attacks much faster ($3 \sim 6\times$) than Basic Attack with a modified binary search does. Although Basic Attack achieves smaller perturbations than AdaptiveAttack does, it is reasonable for binary search method to have a finer tuning on the λ if the initial λ value is properly set and binary search step is large enough.

4.3 Sequential Attack Analysis

To dig into the phenomenon of sequential adversarial examples, we generate adversarial examples on a simple sequential classification task. We first simulate a sequential digit dataset by concatenating digit images in the MNIST dataset [54] and fit them into a 32×100 pixel box. The training and test sequential digits are generated from MNIST training and test datasets. We refer to this dataset as *SeqMNIST*. The first row in Figure 3 illustrates an example (‘24500’) in the *SeqMNIST* dataset. We then trained our model with the training set of *SeqMNIST*.

To analyze the phenomenon of CTC alignments, we consider three types of common adversarial operations on targeted sequential labels: insertion, substitution, and deletion. We perform these operations on one digit and remain the rest unchanged. We also include another operation which inserts a repeated digit (e.g., inserting a ‘5’ from ‘24500’ to ‘245500’). We perform an adversarial attack on the *SeqMNIST* dataset and exam 100 adversarial images for each operation.

CTC alignments in the adversarial examples. We observe that most CTC alignments are stable against adversarial examples (Figure 3). When added perturbations on the images, only the CTC alignments surrounding the targeted labels will be changed. Our observation on four operations are as follows:

- **Insertion:** When inserting a digit into the targeted label, we find that the added perturbations usually appear in the middle of two adjacent digits. Sometimes, it is close to one side so that the new digit can ‘borrow’ some pixels from its neighbor to create itself, which costs smaller perturbations. However, it is not the case for repeated insertions.
- **Insertion (repeated):** The added perturbations usually appear far from the repeated digit. In Figure 3, for instance, the new ‘5’ is close to ‘0’ and

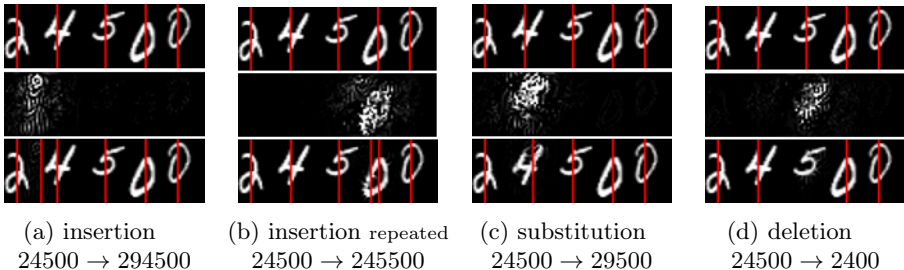


Fig. 3: **Adversarial examples on the *SeqMNIST* dataset.** We perform four types of operations of adversarial attacks: insertion, insertion (repeat), substitution, and deletion. The images in the first row are the same original images. After injecting perturbations (amplified by $10\times$, second row), we generate the adversarial images (third row), which can be misclassified as different labels. Red lines illustrate the corresponding CTC alignments of original labels and targeted labels. In our model, there are 25 alignment positions each representing 4 pixels in width.

far from ‘5’. One explanation is due to the setting of CTC alignment and the operation \mathcal{B} mentioned before: if the perturbations representing the repeated digit is added next to the original digit, the CTC alignment will merge them into one. To successfully inserting a repeated digit, we should have at least one ‘blank’ label between two repeated digits to avoid merging. ‘Blank’ label can be easily generated with the background. For the repeated digit insertion, similar to the insertion case, the adversarial perturbations will be small if we borrow pixel from the other side instead of the original digit. In our experiment setting, This becomes a more efficient and optimal solution.

- **Substitution:** When substituting a label, we observe that the CTC alignments change slightly in the position of substitution. The rest of the targeted labels remain the same positions.
- **Deletion:** When we delete the targeted digit, the remaining CTC alignments barely change their positions. It also requires the least magnitude of perturbations.

To quantify our observations on CTC alignments, we evaluate the edit (Levenshtein) distance between the unaligned original and targeted labels. For example, the edit distance of inserting a ‘9’ (Figure 3a) is 1. The unaligned label changes from ‘-2----4----5----0---0---’ to ‘-2--9-4-----5----0---0---’. The edit distance measures the changed made on the CTC alignments. Deletion operation requires fewer perturbations (1.07) on CTC alignments while the perturbations on Insertion and Insertion (repeated) operations are the largest ones (1.45, 1.44).

4.4 How do attackers generate perturbations iteratively?

We look into the process of generating adversarial examples (Figure 4). The adversarial perturbations are firstly added to the edges of digits surrounding the

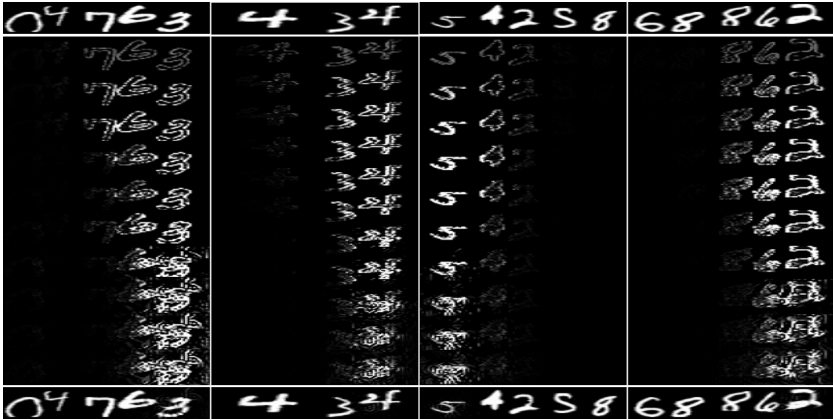


Fig. 4: **Process of iteratively attacking.** We demonstrate four adversarial examples on the *SeqMNIST* dataset. These four examples include insertion ('04763' \rightarrow '047673'), insertion repeated ('434' \rightarrow '4334'), substitution ('54258' \rightarrow '94258'), and deletion ('68862' \rightarrow '6886'). First row: original images. Last row: adversarial images. The middle rows: adversarial perturbations (amplified by $10\times$) added on the original images in the order of iterations.

targeted positions (the new positions based on various adversarial operations), because the gradients of these pixels are larger than the others. The CTC alignments will be aligned to the targeted positions very quickly (in most cases, less than 100 iterations). After the CTC alignments get stable, the CTC alignments will not be changed. The later changes in the images are only to minimize the adversarial perturbations while keeping the prediction unchanged. In a few iterations, the adversarial perturbations look similar to the targeted digits. In the final iteration, it will be minimized to an 'abstract' version of targeted digits, which can not be recognized by humans.

Based on previous observations, **CTC alignments only change in the first few iterations and appear close to the targeted (inserted/ substituted/ deleted) positions.** After that, the adversarial attack will focus on minimizing the magnitude of perturbations.

5 Conclusions

We proposed a novel approach to directly learn multi-task weights without manually tuning the hyper-parameters. The proposed AdaptiveAttack method largely speeds up the process of generating adversarial examples. We successfully attacked a popular scene text recognition system with over 99.9% success rate on three standard benchmark datasets. Visualization analysis of CTC alignments and permutations illustrated attack patterns for sequential learning. Our future work will investigate the defensive mechanisms against sequential adversarial examples.

References

1. Krizhevsky, A., Sutskever, I., Hinton, G.E.: Imagenet classification with deep convolutional neural networks. In: Advances in neural information processing systems. (2012) 1097–1105
2. Simonyan, K., Zisserman, A.: Very deep convolutional networks for large-scale image recognition. arXiv preprint arXiv:1409.1556 (2014)
3. Ren, S., He, K., Girshick, R., Sun, J.: Faster r-cnn: Towards real-time object detection with region proposal networks. In: Advances in neural information processing systems. (2015) 91–99
4. Liu, W., Anguelov, D., Erhan, D., Szegedy, C., Reed, S., Fu, C.Y., Berg, A.C.: Ssd: Single shot multibox detector. In: European conference on computer vision, Springer (2016) 21–37
5. Tian, Z., Huang, W., He, T., He, P., Qiao, Y.: Detecting text in natural image with connectionist text proposal network. In: European conference on computer vision, Springer (2016) 56–72
6. He, P., Huang, W., He, T., Zhu, Q., Qiao, Y., Li, X.: Single shot text detector with regional attention
7. Saon, G., Kuo, H.K.J., Rennie, S., Picheny, M.: The ibm 2015 english conversational telephone speech recognition system. arXiv preprint arXiv:1505.05899 (2015)
8. Szegedy, C., Zaremba, W., Sutskever, I., Bruna, J., Erhan, D., Goodfellow, I., Fergus, R.: Intriguing properties of neural networks. arXiv preprint arXiv:1312.6199 (2013)
9. Goodfellow, I.J., Shlens, J., Szegedy, C.: Explaining and harnessing adversarial examples. arXiv preprint arXiv:1412.6572 (2014)
10. Papernot, N., McDaniel, P., Jha, S., Fredrikson, M., Celik, Z.B., Swami, A.: The limitations of deep learning in adversarial settings. In: Security and Privacy (EuroS&P), 2016 IEEE European Symposium on, IEEE (2016) 372–387
11. Carlini, N., Wagner, D.: Towards evaluating the robustness of neural networks. In: Security and Privacy (S&P), 2017 IEEE Symposium on, IEEE (2017) 39–57
12. Kurakin, A., Goodfellow, I., Bengio, S.: Adversarial examples in the physical world. arXiv preprint arXiv:1607.02533 (2016)
13. Athalye, A., Carlini, N., Wagner, D.: Obfuscated gradients give a false sense of security: Circumventing defenses to adversarial examples. arXiv preprint arXiv:1802.00420 (2018)
14. Carlini, N., Wagner, D.: Adversarial examples are not easily detected: Bypassing ten detection methods. AISEC (2017)
15. Carlini, N., Wagner, D.: Audio adversarial examples: Targeted attacks on speech-to-text. arXiv preprint arXiv:1801.01944 (2018)
16. Graves, A., Fernández, S., Gomez, F., Schmidhuber, J.: Connectionist temporal classification: labelling unsegmented sequence data with recurrent neural networks. In: Proceedings of the 23rd international conference on Machine learning, ACM (2006) 369–376
17. Kendall, A., Gal, Y., Cipolla, R.: Multi-task learning using uncertainty to weigh losses for scene geometry and semantics. In: Proceedings of the IEEE Conference on Computer Vision and Pattern Recognition (CVPR). (2018)
18. Kendall, A., Gal, Y.: What uncertainties do we need in bayesian deep learning for computer vision? In: Advances in neural information processing systems. (2017) 5574–5584

19. Sharif, M., Bhagavatula, S., Bauer, L., Reiter, M.K.: Accessorize to a crime: Real and stealthy attacks on state-of-the-art face recognition. In: Proceedings of the 2016 ACM SIGSAC Conference on Computer and Communications Security, ACM (2016) 1528–1540
20. Huang, S., Papernot, N., Goodfellow, I., Duan, Y., Abbeel, P.: Adversarial attacks on neural network policies. arXiv preprint arXiv:1702.02284 (2017)
21. Kos, J., Song, D.: Delving into adversarial attacks on deep policies. ICLR Workshop (2017)
22. Xie, C., Wang, J., Zhang, Z., Zhou, Y., Xie, L., Yuille, A.: Adversarial examples for semantic segmentation and object detection. In: International Conference on Computer Vision, IEEE (2017)
23. Fischer, V., Kumar, M.C., Metzen, J.H., Brox, T.: Adversarial examples for semantic image segmentation. ICLR 2017 workshop (2017)
24. Hendrik Metzen, J., Chaithanya Kumar, M., Brox, T., Fischer, V.: Universal adversarial perturbations against semantic image segmentation. In: Proceedings of the IEEE Conference on Computer Vision and Pattern Recognition. (2017) 2755–2764
25. Cisse, M., Adi, Y., Neverova, N., Keshet, J.: Houdini: Fooling deep structured prediction models. arXiv preprint arXiv:1707.05373 (2017)
26. Li, J., Monroe, W., Jurafsky, D.: Understanding neural networks through representation erasure. arXiv preprint arXiv:1612.08220 (2016)
27. Jia, R., Liang, P.: Adversarial examples for evaluating reading comprehension systems. In: Proceedings of the Conference on Empirical Methods in Natural Language Processing (EMNLP). (2017)
28. Song, Y., Kim, T., Nowozin, S., Ermon, S., Kushman, N.: Pixeldefend: Leveraging generative models to understand and defend against adversarial examples. In: International Conference on Learning Representations. (2018)
29. Gilmer, J., Metz, L., Faghri, F., Schoenholz, S.S., Raghu, M., Wattenberg, M., Goodfellow, I.: Adversarial spheres. ICLR workshop (2018)
30. Schmidt, L., Santurkar, S., Tsipras, D., Talwar, K., Mądry, A.: Adversarially robust generalization requires more data. arXiv preprint arXiv:1804.11285 (2018)
31. Fawzi, A., Fawzi, H., Fawzi, O.: Adversarial vulnerability for any classifier. arXiv preprint arXiv:1802.08686 (2018)
32. Almazán, J., Gordo, A., Fornés, A., Valveny, E.: Word spotting and recognition with embedded attributes. IEEE transactions on pattern analysis and machine intelligence **36**(12) (2014) 2552–2566
33. Jaderberg, M., Simonyan, K., Vedaldi, A., Zisserman, A.: Synthetic data and artificial neural networks for natural scene text recognition. arXiv preprint arXiv:1406.2227 (2014)
34. Jaderberg, M., Simonyan, K., Vedaldi, A., Zisserman, A.: Deep structured output learning for unconstrained text recognition. arXiv preprint arXiv:1412.5903 (2014)
35. Su, B., Lu, S.: Accurate scene text recognition based on recurrent neural network. In: Asian Conference on Computer Vision, Springer (2014) 35–48
36. He, P., Huang, W., Qiao, Y., Loy, C.C., Tang, X.: Reading scene text in deep convolutional sequences. (2016)
37. Shi, B., Bai, X., Yao, C.: An end-to-end trainable neural network for image-based sequence recognition and its application to scene text recognition. IEEE transactions on pattern analysis and machine intelligence **39**(11) (2017) 2298–2304
38. Hochreiter, S., Schmidhuber, J.: Long short-term memory. Neural computation **9**(8) (1997) 1735–1780

39. Lee, C.Y., Osindero, S.: Recursive recurrent nets with attention modeling for ocr in the wild. In: Proceedings of the IEEE Conference on Computer Vision and Pattern Recognition (CVPR). (2016)
40. Shi, B., Wang, X., Lyu, P., Yao, C., Bai, X.: Robust scene text recognition with automatic rectification. In: Proceedings of the IEEE Conference on Computer Vision and Pattern Recognition (CVPR). (2016)
41. Wei Liu, Chaofeng Chen, K.Y.K.W.Z.S., Han, J.: Star-net: A spatial attention residue network for scene text recognition. In: Proceedings of the British Machine Vision Conference (BMVC). (2016)
42. Jaderberg, M., Simonyan, K., Zisserman, A., et al.: Spatial transformer networks. In: Advances in neural information processing systems. (2015) 2017–2025
43. Biggio, B., Roli, F.: Wild patterns: Ten years after the rise of adversarial machine learning. arXiv preprint arXiv:1712.03141 (2017)
44. Rozsa, A., Rudd, E.M., Boulton, T.E.: Adversarial diversity and hard positive generation. In: Proceedings of the IEEE Conference on Computer Vision and Pattern Recognition (CVPR) Workshops. (2016) 25–32
45. Engstrom, L., Tsipras, D., Schmidt, L., Madry, A.: A rotation and a translation suffice: Fooling cnns with simple transformations. arXiv preprint arXiv:1712.02779 (2017)
46. Sharif, M., Bauer, L., Reiter, M.K.: On the suitability of l_p -norms for creating and preventing adversarial examples. arXiv preprint arXiv:1802.09653 (2018)
47. Yuan, X., He, P., Zhu, Q., Bhat, R.R., Li, X.: Adversarial examples: Attacks and defenses for deep learning. arXiv preprint arXiv:1712.07107 (2017)
48. Papernot, N., McDaniel, P.D., Goodfellow, I.J.: Transferability in machine learning: from phenomena to black-box attacks using adversarial samples. CoRR **abs/1605.07277** (2016)
49. Chen, P.Y., Zhang, H., Sharma, Y., Yi, J., Hsieh, C.J.: Zoo: Zeroth order optimization based black-box attacks to deep neural networks without training substitute models. arXiv preprint arXiv:1708.03999 (2017)
50. Kingma, D., Ba, J.: Adam: A method for stochastic optimization. arXiv preprint arXiv:1412.6980 (2014)
51. Wang, K., Babenko, B., Belongie, S.: End-to-end scene text recognition. In: Computer Vision (ICCV), 2011 IEEE International Conference on, IEEE (2011) 1457–1464
52. Karatzas, D., Shafait, F., Uchida, S., Iwamura, M., i Bigorda, L.G., Mestre, S.R., Mas, J., Mota, D.F., Almazan, J.A., De Las Heras, L.P.: Icdar 2013 robust reading competition. In: Document Analysis and Recognition (ICDAR), 2013 12th International Conference on, IEEE (2013) 1484–1493
53. Mishra, A., Alahari, K., Jawahar, C.V.: Scene text recognition using higher order language priors. In: BMVC. (2012)
54. LeCun, Y., Cortes, C., Burges, C.: The mnist data set (1998)